The hypothesis of the local supercloud and the nearby moving groups of stars

C. A. Olano⋆†

Facultad de Ciencias Astronómicas y Geofísicas, Universidad Nacional de La Plata, Paseo del Bosque, 1900 La Plata, Argentina

ABSTRACT

The velocity distribution of stars in the solar neighbourhood can be globally characterized by the presence of two stellar streams (I and II). Stream I contains kinematic substructures, named moving groups of stars, such us the Pleiades and Hyades groups. While Stream II is essentially associated with the Sirius group. The origin and nature of these two stellar streams are still not completely clear. We propose that Streams I and II were gravitationally linked to an old gas supercloud that was disintegrated in parts that formed new subsystems, viz., the Orion arm and Gould's belt. On the basis of this idea, we constructed a dynamical model of the supercloud in order to explain the kinematic and structural characteristics of the local system of gas and stars. For the study of the relative orbits of the two stellar streams with respect to the supercloud's centre and of the Galactic orbit of the supercloud, we developed appropriate epicyclic motion equations. The results of the model indicate the possibility that about 75–100 Myr ago the supercloud crossed the Perseus arm and as a consequence was strongly braked. Besides, around 60 Myr ago, the position of the supercloud coincided approximately with that of the Big Dent, a huge depression of the Galactic disc. We suggest that the cause that originated the Big Dent could be the same that perturbed the supercloud starting the formation of the Orion arm and Gould's belt. In this context, we derived the theoretical distributions of positions and velocities for the stars of Streams I and II.

Key words: stars: kinematics and dynamics – ISM: clouds – Galaxy: kinematics and dynamics – local interstellar matter – open clusters and associations: individual: Gould's belt; Orion arm; Sirius, Pleiades and Hyades moving groups – solar neighbourhood.

1 INTRODUCTION

The solar neighbourhood within 1 kpc contains structures, such as the local (Orion) arm, Gould's belt and moving stellar groups, which would not been independent of each other. The thesis of this study is that this local system of gas and stars would be the result of an old supercloud in advanced state of disintegration, and interestingly the Sun itself could have been connected for a long time with this supercloud. The understanding of the relationships among these different subsystems can help us to reconstruct globally the evolutionary history of the supercloud, which, in turn, might be linked to the occurrence of certain geological and biological events along the terrestrial history (e.g. Clube & Napier 1982, 1986; de la Fuente Marcos & de la Fuente Marcos 2004). We can think of the progenitor supercloud of the local system as having a diameter of ∼600 pc and a mass of ∼2 × 10⁷ M⊙ (Olano 2015), which is within the characteristics of the superclouds found in our Galaxy

and in external galaxies (Elmegreen & Elmegreen 1983; Efremov 2010).

The Orion arm and Gould's belt are relatively young (<100 Myr old), and probably products of a strong interaction of the supercloud with the interstellar medium during the last 100 Myr. Comprehensive reviews on this topic are given by Pöppel (1997) and Bobylev (2014). On the other hand, the ages of moving stellar groups are much greater, where the more conspicuous ones have approx. 400–600 Myr and probably are related with the origin of the supercloud (Olano 2001). For instance, the ages of the Sirius group and of the Hyades group are 350–413 Myr and 488–679 Myr, respectively (Bovy & Hogg 2010). The age heterogeneity observed in certain moving groups (De Simone, Wu & Tremaine 2004; Famaey et al. 2005; Famaey, Siebert & Jorissen 2008) could imply that an important stellar component of the supercloud contains field stars captured by the supercloud in its origin (Olano 2015). There are some moving groups that are very old, with mean stellar ages greater than 3 Gyr (Bobylev, Bajkova & Mylläri 2010), and their kinematic association with the main groups could also be explained by a capture mechanism. The exception would be the Arcturus group, whose very high velocity (≈100 km s⁻¹) could imply that this group forms part

⋆ E-mail: colano@fcaglp.fcaglp.unlp.edu.ar

† Member of The Carrera del Investigador Científico, CONICET, Argentina.

of the solar neighbourhood extension of the thick disc population (Navarro, Helmi & Freeman 2004). The nearby moving groups have been historically characterized as belonging to two stellar streams, viz., Stream I and Stream II (Kapteyn 1905)

On the idea that the stellar Streams I and II are the remnants of an originally giant complex of gas and stars, we will attempt to reconstruct broadly the events that led, on the one hand, to the disintegration of the old supercloud, and on the other hand, to the formation of new subsystems, viz., the Orion arm and Gould's belt. The paper is organized in the following way. In Section 2, we give a detailed deduction of the epicyclical equations of motion for clouds and stars of the Galaxy, considering that the Galaxy has a flat rotation curve and that the gas clouds can be also subjected to non-gravitational forces. First, we develop the epicyclic equations describing the motion of an interstellar gas cloud, not necessarily in quasi-circular orbit, with respect to a reference system in circular Galactic orbit (Section 2.1). Secondly, we develop the epicyclic equations describing the motions of the stars, bounded gravitationally to the gas cloud, relative to its gravitational centre (Section 2.2). In Section 3, we postulate the evolutive and physical conditions of the local supercloud; and apply the epicyclical equations to determine the orbits of the supercloud and of Stream II (Section 3.1), and the orbits of the supercloud's nucleus and of Stream I (Section 3.2). In Section 4, from the supercloud's model, we derive different spatial and velocity distributions of Streams I and II, which can be compared with the observational distributions. In Section 5, we discuss the effects of certain variations of the supercloud's model on the results. Finally, in Section 6, we give the conclusions.

2 EPICYCLIC EQUATIONS OF MOTION TO CALCULATE RELATIVE ORBITS IN THE GALAXY

The epicyclic formulation has been very useful for the study of dynamics of different Galactic systems (Bok 1934; Mineur 1939; Lindblad 1941; Chandrasekhar 1942). The classical epicyclic equations of motion are obtained under the assumption that we are dealing with quasi-circular orbits. Hence, our first aim is to obtain exact epicyclic equations for general orbits, and then to evaluate the simplification of these equations under specific conditions.

2.1 Supercloud's orbit relative to a local reference system in Galactic rotation

We will use two Cartesian coordinate systems on the Galactic plane. The first one is defined by a stationary frame (x, y) with origin at the Galactic centre (Gc). The second one is defined by a rotating frame (η, ξ) whose coordinate origin lies at a distance R_0 from Gc and describes a circular orbit about Gc with a constant angular velocity ω_0. The positive η-axis points in the rotation direction and the positive ξ-axis points in the anti-centre direction (see Fig. 1). We will study the orbit of a mass point C, moving on the Galactic plane under the central gravitational force $K(R_c)$ of the Galaxy, which is a function of the Galactocentric distance of the point C, here denoted by R_c. The mass point C can represent for instance the gravitational centre of a gas-star complex (in our case, the local supercloud, see Fig. 1). Besides, we assume that the mass point C is under the action of an arbitrary additional force F (per unit mass) that is not gravitational and acts on the gas component of the supercloud. In our case, F will represent an hydrodynamic force due to the friction between the gas supercloud and the surrounding interstellar medium or due to the pass of a shock
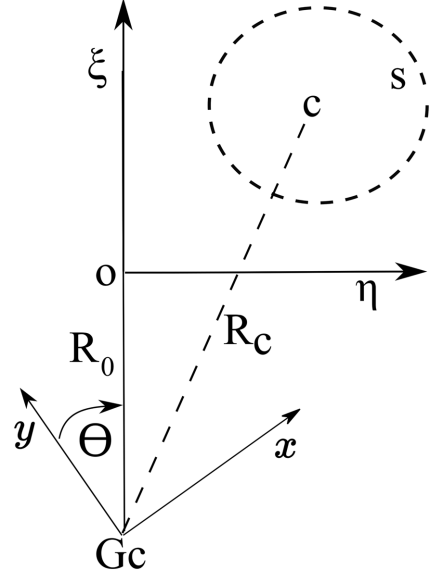
Figure 1. Illustration of the stationary coordinate system (x, y) centred at the Galactic centre and the rotating coordinate system (η, ξ) of origin O moving on a circular orbit of radius R_0. The figure plane represents the Galactic plane and the rotation sense is clockwise. The angle θ, between the y-axis and ξ-axis, increases in the sense of the Galactic rotation.

wave that affects the gas supercloud. Then, the motion equations in the reference system (x, y) are given by

$$\ddot{x}_c = -K(R_c)\frac{x_c}{R_c} + F_x$$
$$\ddot{y}_c = -K(R_c)\frac{y_c}{R_c} + F_y, \tag{1}$$

where F_x and F_y are the components of F and subscript c refers to the coordinates of the point C. Because the force $K(R_c)$ is equal to the centripetal force at R_c, we will write $K(R_c) = R_c\,\omega(R_c)^2$, where $\omega(R_c)$ refers to the Galactic angular velocity at R_c and for short will be written as ω_c. Since we are interested in referring the motions to the rotating system, we should convert equations (1) into ones depending on (η, ξ). The formulae that govern this transformation are

$$x_c = (R_0 + \xi_c)\sin\theta + \eta_c\cos\theta$$
$$y_c = (R_0 + \xi_c)\cos\theta - \eta_c\sin\theta, \tag{2}$$

which are obtained from simple geometrical considerations of Fig. 1. Besides, we should have into account that $F_x = F_\xi\sin\theta + F_\eta\cos\theta$ and $F_y = F_\xi\cos\theta - F_\eta\sin\theta$, and that θ is a function of time t given by $\theta = \theta_0 + \omega_0 t$. We adopt $\theta_0 = 0$, i.e. the y-axis and ξ-axis agree at $t = 0$. Differentiating twice equations (2) with respect to the time t, we obtain

$$\ddot{x}_c = a_1\cos\theta + a_2\sin\theta$$
$$\ddot{y}_c = -a_1\sin\theta + a_2\cos\theta, \tag{3}$$

where $a_1 = \ddot{\eta}_c + 2\omega_0\dot{\xi}_c - \omega_0^2\eta_c$ and $a_2 = \ddot{\xi}_c - 2\omega_0\dot{\eta}_c - \omega_0^2(R_0 + \xi_c)$. From the second members of equations (1), with the corresponding replacements, we get that

$$\ddot{x}_c = c_1\cos\theta + c_2\sin\theta$$
$$\ddot{y}_c = -c_1\sin\theta + c_2\cos\theta, \tag{4}$$

where $c_1 = -\eta_c\,\omega_c^2 + F_\eta$ and $c_2 = -(R_0 + \xi_c)\,\omega_c^2 + F_\xi$. By equating equations (3) to the corresponding equations (4), we have

$$a_1\cos\theta + a_2\sin\theta = c_1\cos\theta + c_2\sin\theta$$
$$-a_1\sin\theta + a_2\cos\theta = -c_1\sin\theta + c_2\cos\theta. \qquad (5)$$

The system of equations (5) is equivalent to the system $a_1 = c_1$ and $a_2 = c_2$. Thus, the exact epicyclic equations of motion for the mass point C are

$$\ddot{\eta}_c + 2\omega_0\,\dot{\xi}_c + (\omega_c^2 - \omega_0^2)\,\eta_c = F_\eta$$
$$\ddot{\xi}_c - 2\omega_0\,\dot{\eta}_c + (\omega_c^2 - \omega_0^2)\,R_0 + (\omega_c^2 - \omega_0^2)\,\xi_c = F_\xi. \qquad (6)$$

If we adopt a flat rotation curve for the Galaxy, with a rotation velocity $V_0 = 220\,\mathrm{km\,s^{-1}}$, in approximate agreement with the measurements in a large range of Galactocentric distances (e.g. Sofue, Honma & Omodaka 2009; Bovy et al. 2012), $\omega_c = \frac{V_0}{R_c}$ and $\omega_0 = \frac{V_0}{R_0} = \mathrm{const}$. Since $R_c^2 = (R_0 + \xi_c)^2 + \eta_c^2$ (see Fig. 1), we have

$$\omega_c = \frac{V_0}{\sqrt{(R_0 + \xi_c)^2 + \eta_c^2}}. \qquad (7)$$

For the study of the orbit of the local supercloud, the origin of the system (η, ξ) should be located in the solar neighbourhood at the Galactocentric distance of the Sun (i.e. $R_0 \approx 8$ kpc). Replacing equation (7) into equations (6), this equation system can be solved numerically.

The initial conditions needed to solve the differential equation system (6), i.e. $\eta_c(0)$, $\xi_c(0)$, $\dot{\eta}_c(0)$, $\dot{\xi}_c(0)$, will be calculated from the LSR velocity and position of the supercloud's gravitational centre at $t = 0$. With this purpose, we use the relations (2) to obtain $\eta_c = x_c\cos\theta - y_c\sin\theta$ and $\xi_c = x_c\sin\theta + y_c\cos\theta - R_0$. Hence, $\dot{\eta}_c = -\omega_0 x_c\sin\theta - \omega_0 y_c\cos\theta + \dot{x}_c\cos\theta - \dot{y}_c\sin\theta$ and $\dot{\xi}_c = \omega_0 x_c\cos\theta - \omega_0 y_c\sin\theta + \dot{x}_c\sin\theta + \dot{y}_c\cos\theta$. Since $\theta = \omega_0 t = 0$ at $t = 0$, the former formulae give $\eta_c(0) = x_c(0)$, $\xi_c(0) = y_c(0) - R_0$ and

$$\dot{\eta}_c(0) = -\omega_0\xi_c(0) + \dot{X}_c(\mathrm{LSR})$$
$$\dot{\xi}_c(0) = \omega_0\eta_c(0) + \dot{Y}_c(\mathrm{LSR}), \qquad (8)$$

where $\dot{X}_c(\mathrm{LSR}) = \dot{x}_c(0) - \omega_0 R_0$ and $\dot{Y}_c(\mathrm{LSR}) = \dot{y}(0)$, which correspond to the LSR velocity components. The positive axis of $\dot{X}_c(\mathrm{LSR})$ velocities points in the direction of the Galactic rotation and the positive axis of $\dot{Y}_c(\mathrm{LSR})$ velocities points in the direction opposite to that of the Galactic centre.

It also is of interest to calculate from the values of $\eta_c(t)$, $\xi_c(t)$, $\dot{\eta}_c(t)$ and $\dot{\xi}_c(t)$ at a certain time t, the corresponding LSR-velocity. Projecting the velocities components $\dot{x}_c$ and $\dot{y}_c$ on to the radio vector R_c and a direction perpendicular to this vector, the LSR velocity of the supercloud's centre at the position $(\eta_c(t), \xi_c(t))$, or at $R_c(= \sqrt{(R_0 + \xi_c(t))^2 + \eta_c(t)^2}\,)$, is given by

$$\dot{X}_c(\mathrm{LSR}) = \dot{x}_c\cos A - \dot{y}_c\sin A - V_0$$
$$\dot{Y}_c(\mathrm{LSR}) = \dot{x}_c\sin A + \dot{y}_c\cos A, \qquad (9)$$

where A is the angle between the y-axis and the radio vector R_c, and hence $A = \theta + \alpha$, where $\alpha = \arctan\frac{\eta_c(t)}{R_0 + \xi_c(t)}$ (Fig. 1). The expressions of $\dot{x}_c$ and $\dot{y}_c$ used in (9) are functions of $\eta_c(t)$, $\xi_c(t)$, $\dot{\eta}_c(t)$ and $\dot{\xi}_c(t)$, obtained by means of equations (2). Note that if α is small as compared to θ, equations (9) become

$$\dot{X}_c(\mathrm{LSR}) \simeq \dot{\eta}_c(t) + \omega_0\xi_c(t)$$
$$\dot{Y}_c(\mathrm{LSR}) \simeq \dot{\xi}_c(t) - \omega_0\eta_c(t), \qquad (10)$$

and equations (8) are a particular case of equations (10).

2.2 Orbits of the supercloud's stars relative to the gravitational centre of the supercloud

The aim of this section is to determine the orbit of a star S with respect to the gravitational centre C of a gas-star complex in the rotating system (η, ξ) (see Fig. 1). We assume that the star S is subject to the general Galactic gravitational force, $K(R_s) = R_s\,\omega(R_s)^2$, and to a central gravitational force due to the supercloud, $J(r)$, where R_s is the Galactocentric distance of the star S, r is the distance of the star S from C, and the subscript S refers to the star S. The components of the force $J(r)$ are therefore $J_\eta = J(r)\frac{\eta_s - \eta_c}{r}$ and $J_\xi = J(r)\frac{\xi_s - \xi_c}{r}$, where $r = \sqrt{(\eta_s - \eta_c)^2 + (\xi_s - \xi_c)^2}$. By analogy with the system of equations (6), the motion equations for the star S are

$$\ddot{\eta}_s + 2\omega_0\,\dot{\xi}_s + (\omega_s^2 - \omega_0^2)\,\eta_s = J_\eta$$
$$\ddot{\xi}_s - 2\omega_0\,\dot{\eta}_s + (\omega_s^2 - \omega_0^2)\,R_0 + (\omega_s^2 - \omega_0^2)\,\xi_s = J_\xi. \qquad (11)$$

The solution of the system of coupled differential equations (11) requires that we first or simultaneously solve the system of coupled differential equations (6) for η_c and ξ_c. Then, the relative orbit of S with respect to C is simply given by $\eta^\star(t) = \eta_s(t) - \eta_c(t)$ and $\xi^\star(t) = \xi_s(t) - \xi_c(t)$, where the symbol $\star$ for the superscript of the coordinates refers to the relative orbit with respect to the supercloud's centre.

The epicyclical equations of motion given by equations (6) and (11) are greatly simplified by means of the approximation $R_c \approx R_0 + \xi_c$ and $R_s \approx R_0 + \xi_s$, which is valid if the coordinates η and ξ of the C and S are small with respect to R_0. This simplification leads to the classical epicyclical equations. In effect, $(\omega_c^2 - \omega_0^2) = (\frac{V_0}{R_c})^2 - (\frac{V_0}{R_0})^2 = -\omega_0^2\frac{(R_0 + R_c)(R_c - R_0)}{R_c^2} \approx -\omega_0^2\frac{(2R_0 + \xi_c)\xi_c}{(R_0 + \xi_c)^2} \approx -2\omega_0^2\frac{\xi_c}{R_0}$, with which equations (6) become

$$\ddot{\eta}_c + 2\omega_0\,\dot{\xi}_c + \epsilon_c = F_\eta \qquad (12)$$

$$\ddot{\xi}_c - 2\omega_0\,\dot{\eta}_c - 2\omega_0^2\,\xi_c + \delta_c = F_\xi, \qquad (13)$$

where $\epsilon_c = -\frac{2\omega_0^2\xi_c\eta_c}{R_0}$ and $\delta_c = -\frac{2\omega_0^2\xi_c^2}{R_0}$, which can be neglected in this approximation. Similarly, $(\omega_s^2 - \omega_0^2) \approx -2\omega_0^2\frac{\xi_s}{R_0}$, with which equations (11) become

$$\ddot{\eta}_s + 2\omega_0\,\dot{\xi}_s + \epsilon_s = J_\eta \qquad (14)$$

$$\ddot{\xi}_s - 2\omega_0\,\dot{\eta}_s - 2\omega_0^2\,\xi_s + \delta_s = J_\xi, \qquad (15)$$

where $\epsilon_s = -\frac{2\omega_0^2\xi_s\eta_s}{R_0}$ and $\delta_s = -\frac{2\omega_0^2\xi_s^2}{R_0}$.

From former equations, we can derive a system of motion equations to calculate conveniently the relative orbit of S about C. Subtracting term by term equation (12) from equation (14) and equation (13) from equation (15), and remembering that $\eta^\star = \eta_s - \eta_c$ and $\xi^\star = \xi_s - \xi_c$, we obtain the following equation system:

$$\ddot{\eta}^\star + 2\omega_0\,\dot{\xi}^\star = J_\eta - F_\eta$$
$$\ddot{\xi}^\star - 2\omega_0\,\dot{\eta}^\star - 2\omega_0^2\,\xi^\star = J_\xi - F_\xi, \qquad (16)$$

where the higher order terms, ϵ and δ, were neglected. This system of motion equations has the advantage that will permit us to calculate, although approximately, the relative orbits of the supercloud's stars without calculating previously the orbit of gravitational centre C of the supercloud. Note that the forces F_η and F_ξ are reflected with the reverse signs in the system (16) that governs the relative motions of the stars.

In order to obtain the initial conditions for equation (16), we need to find the relationships between the initial velocity and position in the rotating system with the corresponding ones in the LSR system. Subtracting term by term equations (8) from similar equations for S, we get

$$\dot{\eta}^{\star}(0) = -\omega_0 \xi^{\star}(0) + \dot{X}^{\star}(\text{LSR})$$
$$\dot{\xi}^{\star}(0) = \omega_0 \eta^{\star}(0) + \dot{Y}^{\star}(\text{LSR}), \qquad (17)$$

where $\dot{X}^{\star}(\text{LSR}) = \dot{X}_s(\text{LSR}) - \dot{X}_c(\text{LSR})$ and $\dot{Y}^{\star}(\text{LSR}) = \dot{Y}_s(\text{LSR}) - \dot{Y}_c(\text{LSR})$. The initial position $(\eta^{\star}(0), \xi^{\star}(0))$ agrees in both systems, but the initial velocity $(\dot{\eta}^{\star}(0), \dot{\xi}^{\star}(0))$ contains terms due to the system's rotation.

3 THE LOCAL SUPERCLOUD'S MODEL

The final aim of this section is to explain, on the basis of the supercloud model, the particular velocity distribution of the stars in the solar vicinity. The modern determinations of the kinematics of the local stars (Dehnen 1998; Bovy, Hogg & Roweis 2009; Bovy & Hogg 2010; Gontcharov 2012a,b) confirm the existence of the main kinematic stellar groups. On the whole, there are basically two main kinematic structures, the stellar Streams I and II, as classically interpreted (Kapteyn 1905). Stream I includes the Hyades, the Pleiades, NGC 1991 and Hercules moving groups ; and Stream II is associated with the Sirius group, also named Sirius supercluster, which includes the sparse Ursa Major nucleus cluster (Eggen 1998).

We postulate that, during the last 50–100 Myr, the supercloud has been subject to instabilities that dispersed and braked the gaseous component of the supercloud, in part as consequence of a strong interaction with the background interstellar matter. The Orion arm and the Gould belt were formed from the dispersed gas of the supercloud. Because of the stars are not almost affected directly by the interaction with the interstellar medium, the stars associated with the supercloud, i.e. the moving stellar groups, preserve still their dynamical memory. Therefore, the study of the orbits of the moving groups relative to the centre of the hypothetical supercloud in disintegration can help us to reconstruct the orbit of the gaseous part of the supercloud and thus to infer its possible origin.

We represent the supercloud by a uniform ellipsoid of density ρ, semimajor axis a and eccentricity e. We consider that ρ is almost coincident with the density of the gaseous component of the supercloud. In other words, *the mass of the stellar component of the supercloud is considered small, compared to that of the gaseous component, and therefore its gravitational influence on the gas supercloud is negligible*. In order to model the disintegration process of the supercloud, we assume that the density ρ is a function of time given by $\rho(t) = \rho_0(1 + \lambda t)$, where ρ_0 and λ are constant. Hence, the force $J(r)$, defined in Section 2.2, is given by $J(r) = -2\pi G \rho(t) \frac{\sqrt{1-e^2}}{e^2}(\frac{\arcsin e}{e} - \sqrt{1-e^2})\, r$, for $r \leq a$. G is the gravitational constant. Thus, we can write $J_\eta = J(r)\frac{\eta^{\star}}{r} = -k^2(1 + \lambda t)\eta^{\star}$ and $J_\xi = J(r)\frac{\xi^{\star}}{r} = -k^2(1 + \lambda t)\xi^{\star}$, where $k^2 = 2\pi G \rho_0 \frac{\sqrt{1-e^2}}{e^2}(\frac{\arcsin e}{e} - \sqrt{1-e^2})$. Then, the formulae (16) result

$$\ddot{\eta}^{\star} + 2\omega_0 \dot{\xi}^{\star} + k^2(1 + \lambda t)\eta^{\star} = -F_\eta$$
$$\ddot{\xi}^{\star} - 2\omega_0 \dot{\eta}^{\star} - 2\omega_0^2 \xi^{\star} + k^2(1 + \lambda t)\xi^{\star} = -F_\xi. \qquad (18)$$

The force components F_η and F_ξ in equations (18) will represent braking forces acting on the gaseous component of the supercloud due to the interaction with the interstellar matter. We will assume

that F_η and F_ξ are functions of time t that can be expressed in power-series as

$$F_\eta = \sum_{n=0}^{\infty} f\eta_n t^n$$
$$F_\xi = \sum_{n=0}^{\infty} f\xi_n t^n, \qquad (19)$$

where $f\eta_n$ and $f\xi_n$ are the series coefficients.

We will obtain the solution of the differential equation system (18) by means of a power-series method. Writing the solution in the form

$$\eta^{\star} = \sum_{n=0}^{\infty} \eta_n t^n$$
$$\xi^{\star} = \sum_{n=0}^{\infty} \xi_n t^n, \qquad (20)$$

the values of series coefficients that satisfy equations (18) are

$$\eta_2 = \frac{1}{2}(-f\eta_0 - k^2\eta_0 - 2\omega_0\xi_1)$$
$$\xi_2 = \frac{1}{2}(-f\xi_0 - k^2\xi_0 + 2\omega_0\eta_1 + 2\omega_0^2\xi_0), \qquad (21)$$

and for $n \geq 3$

$$\eta_n = \frac{1}{n(n-1)}(-f\eta_{n-2} - k^2\lambda\,\eta_{n-3} - k^2\eta_{n-2} - 2(n-1)\omega_0\xi_{n-1})$$
$$\xi_n = \frac{1}{n(n-1)}\Big(-f\xi_{n-2} - k^2\lambda\,\xi_{n-3} - k^2\xi_{n-2} + 2(n-1)\omega_0\eta_{n-1}$$
$$+ 2\omega_0^2\xi_{n-2}\Big), \qquad (22)$$

where η_0, ξ_0, η_1 and ξ_1 are given by the initial position and velocity. That is to say $\eta_0 = \eta^{\star}(0)$, $\xi_0 = \xi^{\star}(0)$, $\eta_1 = \dot{\eta}^{\star}(0)$ and $\xi_1 = \dot{\xi}^{\star}(0)$.

3.1 Tentative reconstruction of the gaseous supercloud's orbit and of the Stream II's orbit

Our main objective in this section is to trace back in time the orbit of the supercloud and of Stream II associated with the Sirius group, between the present time $t = 0$ and the time $t_d < 0$ in which the disintegration phase of the supercloud started. The main assumption of the model is that the position and velocity of the centroid of Stream II coincided with those of the gravity centre of the supercloud at the beginning of the disintegration process. This assumption is key to the reconstruction of the supercloud's orbit.

Then, making use of the series-solution (20), we can write

$$\eta^{\star}_{II}(t_d) = \sum_{n=0}^{\infty} \eta_n t_d^n = 0$$
$$\xi^{\star}_{II}(t_d) = \sum_{n=0}^{\infty} \xi_n t_d^n = 0$$
$$\dot{\eta}^{\star}_{II}(t_d) = \sum_{n=0}^{\infty} n\eta_n t_d^{n-1} = 0$$
$$\dot{\xi}^{\star}_{II}(t_d) = \sum_{n=1}^{\infty} n\xi_n t_d^{n-1} = 0, \qquad (23)$$

where subscript II refers to Stream II. Besides, we assume here that the force components F_η and F_ξ do not depend on time during the braking process. Then, $f\eta_n = f\xi_n = 0$ for $n \geq 1$.

Substituting $\eta_0 = \eta_{II}^{\star}(0)$, $\xi_0 = \xi_{II}^{\star}(0)$, $\eta_1 = \dot{\eta}_{II}^{\star}(0) = -\omega_0\xi_{II}^{\star}(0) + \dot{X}_{II}^{\star}(LSR)$ and $\xi_1 = \dot{\xi}_{II}^{\star}(0) = \omega_0\eta_{II}^{\star}(0) + \dot{Y}_{II}^{\star}(LSR)$ (cf. equations 17) into equations (21) and (22), and substituting these resulting coefficients into equations (23), we obtain a linear system of four equations with four unknowns, namely: $\eta_{II}^{\star}(0)$, $\xi_{II}^{\star}(0)$, $f\eta_0$ and $f\xi_0$. The relative LSR velocity of the centroid of Stream II with respect to the centre C of the supercloud, i.e. ($\dot{X}_{II}^{\star}(LSR)$, $\dot{Y}_{II}^{\star}(LSR)$), is in principle an observational data.

Note that our $\dot{X}(LSR)$ and $\dot{Y}(LSR)$ velocity components are coherently related with the coordinate system (ξ, η) (equations 9 and 10) in which the epicyclic equations are classically expressed. However, our reference system is different from the conventional Galactic coordinate system (X,Y,Z) and the corresponding U, V and W velocity components, to which the observational data are usually referred. When necessary, we will do the corresponding conversions. We consider that because of the braking process, the present peculiar velocity of the supercloud as a whole is small, and in consequence we adopt $\dot{X}_c(LSR) = 0$ and $\dot{Y}_c(LSR) = 0$. Besides, we consider that LSR velocity of the centroid of Stream II is represented by the centroid of the velocity distribution of the Sirius group. From the velocity distribution of nearby stars determined by Bovy et al. (2009), Bovy & Hogg (2010), we obtain that the X and Y components of the LSR velocity centroid of Stream II are ≈ 10 km s^{-1} and -20 km s^{-1}, respectively, and therefore $\dot{X}_{II}^{\star}(LSR) = 10$ km s^{-1}, and $\dot{Y}_{II}^{\star}(LSR) = -20$ km s^{-1}. This velocity centroid of Stream II was estimated by eye on fig. 1 of Bovy & Hogg (2010) and its velocity was measured relative to the velocity of the LSR, indicated by a triangle in the mentioned figure. In fig. 1 of Bovy & Hogg (2010), the heliocentric velocity components of the stars are denoted by v_x (=U) and v_y (=V), where the positive v_x-axis points towards the galactic longitude $l = 0°$, and the positive v_y-axis towards $l = 90°$. Therefore, the v_x-axis coincides with our $\dot{Y}$-axis, but the positive v_x-axis points in the opposite direction to that of the $\dot{Y}$-axis. The v_y-axis coincides with our $\dot{X}$-axis and both positive axes point in the same direction. In other words, $\dot{X}_{II}^{\star}(LSR)$ is equal to v_y of the centroid minus v_y of the LSR, and $-\dot{Y}_{II}^{\star}(LSR)$ is equal to v_x of the centroid minus v_x of the LSR.

We tentatively fix $t_d = -100$ Myr. We define $\lambda = \frac{\rho_d - \rho_0}{\rho_0}\frac{1}{t_d}$, where ρ_0 and ρ_d are the supercloud's density at $t = 0$ and at $t = t_d$, respectively (see the general presentation of the model in Section 3). We adopt $\rho_0 = 1$ at cm^{-3}, $\rho_d = 14$ at cm^{-3} and $e = 0.86$ (Olano 2015). With the adopted parameters, the solution of the linear equation system stated by the boundary condition (23) gives the following values for its unknowns: $\eta_{II}^{\star}(0) = 569.3$ pc, $\xi_{II}^{\star}(0) = -218.1$ pc, $F_\eta = f\eta_0 = -0.51$ km s^{-1} Myr^{-1} and $F_\xi = f\xi_0 = 0.34$ km s^{-1} Myr^{-1}. Replacing these values into equations (21) and (22), we obtain the values for η_n and ξ_n with which equations (20) give us the relative orbit of Stream II as a whole, by varying t between $t = 0$ and $t = t_d$ (see Figs 2 and 3).

The condition (23) has allowed us to estimate the effective forces that acted on the supercloud, that is, F_η and F_ξ. Therefore, we are now in condition to obtain also the orbit of the centre C of the supercloud during the last 100 Myr. Assuming that the supercloud's centre C is located in the solar neighbourhood, we can place the origin of the coordinate system (η, ξ) at C, and in consequence the initial conditions of C are $\eta_c(0) = 0$, $\xi_c(0) = 0$, $\dot{\eta}_c(0) = 0$ and $\dot{\xi}_c(0) = 0$. With these initial conditions and the values of F_η and F_ξ, we can solve numerically the exact motion equations (6) with ω_c given by equation (7). We can use also the approximate motion equations (12) and (13), which can be solved analytically. The results are shown in Fig. 4.
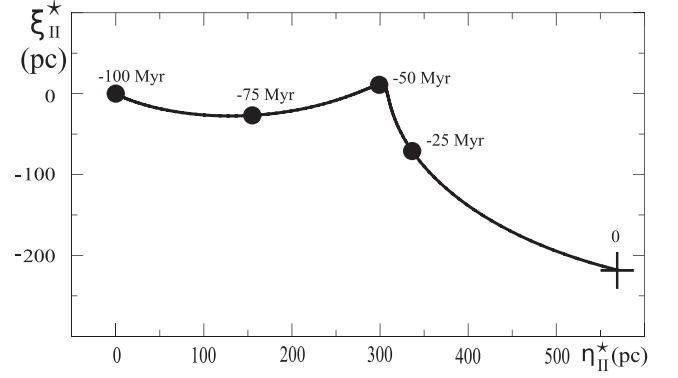
Figure 2. Relative orbit of Stream II as a whole, in the rotating reference system (η, ξ). The cross indicates the present position of the Stream II's centroid with respect to the hypothetical centre of the supercloud. The points show positions at the indicated times
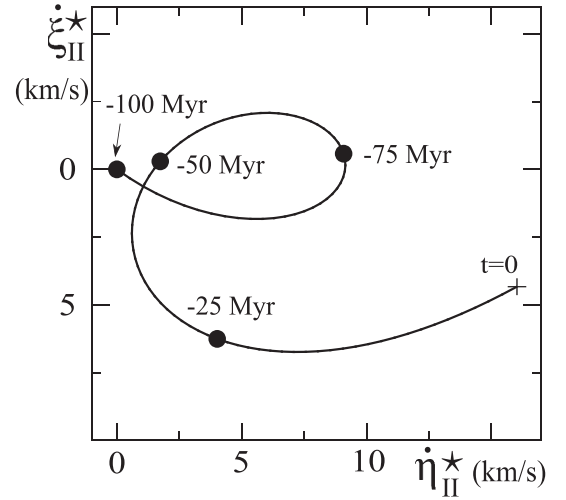

Figure 3. The velocity components along the relative orbit of Stream II as a whole, in the rotating reference system (η, ξ). The points show velocities at the indicated times
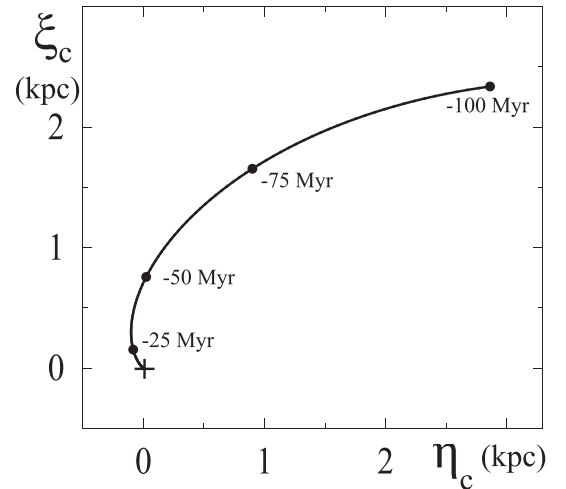
Figure 4. The past orbit of the supercloud's centre, in the rotating reference system (η, ξ). The coordinate origin is placed at the present position of the supercloud's centre, indicated by a cross. Certain positions of the orbit, represented with points, and the corresponding times are noted.
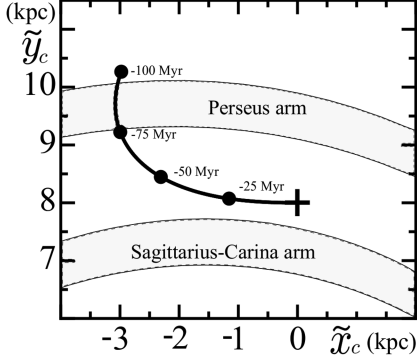
Figure 5. Orbit of the supercloud's centre relative to the nearly spiral arms of the Galaxy. The Galactocentric system $(\tilde{x}, \tilde{y})$ is fixed to the Galactic spiral pattern. The positive $\tilde{x}$-axis points in the direction of the Galactic rotation, and the positive $\tilde{y}$-axis towards the Galactic anticentre. The points on the orbit show the supercloud's positions at the noted times. The cross indicates the present position of the supercloud's centre, which is located in the solar neighbourhood. The picture of the spiral arms was adapted from Vallée (2014).

In order to investigate whether the cause of the braking and destabilization of the supercloud is connected to its passage through a spiral arm, we will determine the relative motion between the supercloud and the spiral structure of the Galaxy. With this aim, the supercloud's orbit will be referred to a Galactocentric system $(\tilde{x}, \tilde{y})$ that rotates with the angular velocity Ω_p of the Galactic spiral pattern. In this reference frame, the spiral pattern is stationary. To convert the positions (η, ξ) of the orbit of the supercloud's centre to the corresponding positions in the frame $(\tilde{x}, \tilde{y})$, we use equations (2) with $\theta = (\omega_0 - \Omega_p)t$. Thus, $\tilde{x}_c(t) = (R_0 + \xi_c(t)) \sin[(\omega_0 - \Omega_p)t] + \eta_c(t) \cos[(\omega_0 - \Omega_p)t]$, and $\tilde{y}_c(t) = (R_0 + \xi_c(t)) \cos[(\omega_0 - \Omega_p)t] - \eta_c(t) \sin[(\omega_0 - \Omega_p)t]$. Modern determinations of Ω_p give values between 20 and 25 km s^{-1} kpc^{-1} (e.g. Junqueira et al. 2015, and references therein). Adopting $\Omega_p = 22$ km s^{-1} kpc^{-1}, and using the positions and their respective times represented in Fig. 4, we obtain the orbit of the supercloud relative to the nearby spiral structure (Fig. 5). This figure shows schematically that the supercloud penetrated into the Perseus arm around 100 Myr ago, which validates the value adopted for t_d ($= -100$ Myr).

In Fig. 6, we draw the X_c and Y_c velocity components of the supercloud with respect to the LSR of the region through which the cloud was passing by, calculated with equations (9). The peculiar velocities represented in Fig. 6 between point A ($t = -200$ Myr) and point B ($t = -100$ Myr) were calculated by tracing back in time the supercloud's orbit with the assumption that friction forces were null in this time interval. At the moment of the encounter of the supercloud with the Perseus arm, the peculiar velocity components of the supercloud were $\dot{X}_c(\text{LSR}) = -12$ km s^{-1} and $\dot{Y}_c(\text{LSR}) = -37$ km s^{-1} (point B). After 25 Myr, the supercloud crossed the arm, reaching the peculiar velocity indicated by the point C. If the supercloud had not been braked by the spiral arm, the peculiar velocity would have been that indicated by the letter C'. This indicates that the supercloud was decelerated in the direction of the Galactic rotation (i.e. the force F_η is negative).

This deceleration of the supercloud can be explained, in principle, within the framework of the density wave theory. The interstellar gas passing through the spiral arm is decelerated by the shock wave associated with the density wave (Roberts 1969), if the Perseus spiral arm is located within the corotation radius (Vallée 2014; Monguió
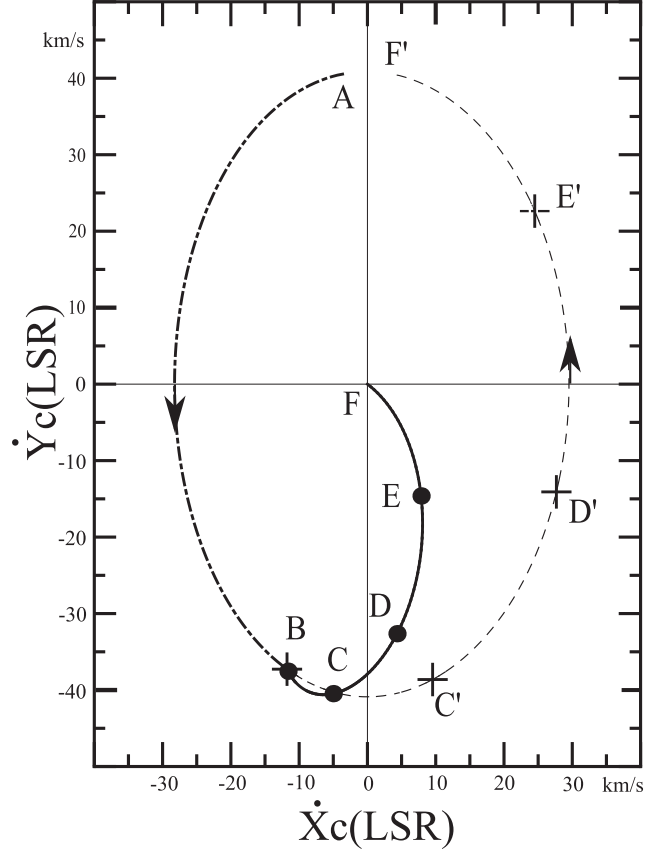
Figure 6. LSR peculiar velocities of the supercloud along its orbit during the last 200 Myr, according to the model A. Points A, B, C, D, E correspond to the times -200, -100, -75, -50 and -25 Myr, respectively. Point F represents the present time. The letters with the prime symbol indicate the peculiar velocities that supercloud would have had, if it had not have braked. The arrows show the temporal direction. The positive axis of the X_c velocity component points in the direction of the Galactic rotation. The positive axis of the Y_c velocity component points towards the Galactic anticentre.

et al. 2015). Congruently, we have chosen $\Omega_p = 22$ km s^{-1} kpc^{-1}, which corresponds to a corotation radius of 10 kpc (see Fig. 5). Our analysis is based on the approach of effective braking forces. However, a detailed analysis should require to study the hydrodynamic interaction between the supercloud and the shock wave associated with the spiral arm.

On the other hand, the force F_ξ was positive and decelerated the supercloud in the ξ − direction, reducing the velocity from -37 km s^{-1} to zero (see Fig. 6). In the first half of the path through the interarm region, the supercloud moved against the stream of the background interstellar gas induced by the spiral density wave, incrementing the velocity of the supercloud relative to the background interstellar gas and consequently the friction or braking force acting on the supercloud. Indeed, in this region, the phase of the density wave varies between $\chi = \pi$ and $\chi = \pi/2$ and consequently the $\tilde{x}$ and $\tilde{y}$ velocity components of the gas streaming motion of the density wave are negative and positive, respectively. Another interesting fact that shows Fig. 5 is that the supercloud's path crosses over a large region of the Galactic disc in which the stars of ages younger than 80 Myr lie below the Galactic plane, structure called Big Dent (Alfaro et al. 1991; Cabrera-Caño et al. 1995). In order to investigate a possible relation of cause and effect, we trace the orbit of the supercloud's centre relative to the centre of the Big Dent
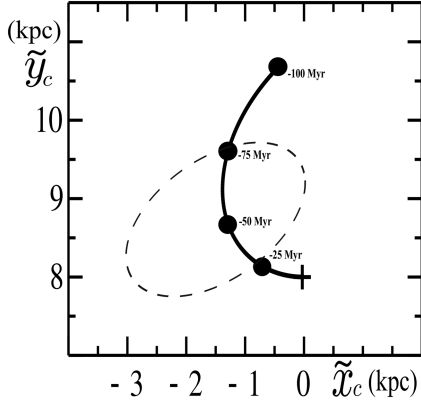
Figure 7. The supercloud's orbit relative to the Big Dent, a large depression of the Galactic disc, whose limit is schematically indicated by a dashed line (cf. fig. 3 of Alfaro, Cabrera-Caño & Delgado 1991).

(Fig. 7). This was obtained by the same procedure we used to obtain Fig. 5, but with $\Omega_p = \frac{220}{R_{BD}}$ km s^{-1} kpc^{-1}, where $R_{BD} = 9$ kpc is the Galactocentric distance of the Big Dent's centre. Fig. 7 shows that the supercloud's centre coincided with the Big Dent's centre around 60 Myr ago. The present size of the Big Dent is represented schematically in Fig. 7. However, this size was probably smaller in the past, since the Big Dent can have been expanding. Therefore, we wonder whether the crossing of the Galactic disc by the supercloud could be the cause of the formation of the Big Dent. Another explanation may be that the falling of an high velocity cloud (HVC) transferred momentum and energy in the Z direction to a part of both gaseous components, of the supercloud and of the Galactic disc, at about 60 Myr ago. Thus, the stars of the Big Dent were formed in the shocked gas layer with a velocity component in the Z-direction (e.g. Comerón & Torra 1992).

3.2 Tentative reconstruction of the orbits of the supercloud's gaseous nucleus and of the associated Stream (I)

We propose that the stars of Stream I were originally bounded to the gaseous nucleus of the supercloud, that is to say the most dense part of the supercloud. We also propose that after crossing the Perseus arm, the supercloud's nucleus suffered in particular the action of a strong force due perhaps to the collision with a dense cloud of peculiar velocity of the Galactic disc. This strong perturbation could in part be induced by the one that originated the Big Dent (see the last paragraph of Section 3.1). Besides we think that, as consequence of this strong force acting on the supercloud's nucleus, the kinematics of the stars of Stream I was greatly affected. In addition, the compression on the gaseous material of the supercloud's nucleus gave origin to Gould's belt. The spatial distribution of O-B stars younger than 100 Myr, projected on the XZ-plane (fig. 3 of Gontcharov 2012a), shows a prominent profile of both structures: the Big Dent and Gould's belt. This notable spatial and temporal coincidence of both structures speaks strongly in favour that their origins are linked.

Various methods to estimate the age of Gould's belt give rather concordant results that indicate an average age of ≈60 Myr (Bobylev 2014). On the basis of the photometric ages of individual stars in Gould's belt, Torra, Fernández & Figueras (2000) estimated that the belt is younger than 60 Myr. Therefore, we will assume that this process of gas compression and star formation started about 60 Myr ago (and probably lasted a period of 10–20 Myr). Because

of the relatively high gas density of the supercloud's nucleus, this nucleus was not greatly affected by the braking forces acting on the whole supercloud in the period between -100 and -60 Myr. Hence, the gaseous nucleus of the supercloud, the stars of Streams I and II shared the same kinematics, until the strong force started to act on a region involving the gaseous nucleus about 60 Myr ago. The components of this additional force will be denoted by N_η and N_ξ. The equations of motion for the supercloud's nucleus, between t=0 and $t = -60$ Myr, can be deduced from considerations similar to those of Section 2.2 (see also Appendix A). Then, we can write

$$\ddot{\eta}_N^\star + 2\omega_0 \dot{\xi}_N^\star + k^2(1 + \lambda\,t)\,\eta_N^\star + f\eta_0 - N_\eta = 0$$
$$\ddot{\xi}_N^\star - 2\omega_0 \dot{\eta}_N^\star - 2\omega_0^2 \xi_N^\star + k^2(1 + \lambda\,t)\,\xi_N^\star + f\xi_0 - N_\xi = 0, \quad (24)$$

where subscript N indicates that we are referring to the supercloud's nucleus. The values for $k, \lambda, f\eta_0$ and $f\xi_0$ are the same we used in the previous section.

Similarly, we can derived the motion equations of Stream I, associated with the gas nucleus of the supercloud (see Appendix A). These equations, in the time interval from 0 to -60 Myr, that govern the motion of Stream I relative to the nucleus' centre result

$$\ddot{\eta}_I^{\star\star} + 2\omega_0 \dot{\xi}_I^{\star\star} + k_N^2(1 + \lambda_N\,t)\,\eta_I^{\star\star} + N_\eta = 0$$
$$\ddot{\xi}_I^{\star\star} - 2\omega_0 \dot{\eta}_I^{\star\star} - 2\omega_0^2 \xi_I^{\star\star} + k_N^2(1 + \lambda_N\,t)\,\xi_I^{\star\star} + N_\xi = 0. \quad (25)$$

The double star superscript indicates that the orbit of Stream I is referred to the nucleus' centre. Hence, by means of $\eta_I^\star(t) = \eta_I^{\star\star}(t) + \eta_N^\star(t)$ and $\xi_I^\star(t) = \xi_I^{\star\star}(t) + \xi_N^\star(t)$, we obtain the Stream I's orbit with respect to the supercloud's centre. Here, $\lambda_N = \frac{N\rho_d - N\rho_0}{N\rho_0}\frac{1}{t_d'}$, where $N\rho_0$ and $N\rho_d$ are the nucleus' density at the present ($t = 0$) and at $t = t_d' = -60$ Myr, respectively (see Section 3.1). We adopt $N\rho_0 = 1$ at cm^{-3}, $N\rho_d = 120$ at cm^{-3} and $e = 0.86$. The constant k_N is the same as k defined in Section 3.1, except that we replace ρ_0 by $N\rho_0$. The value adopted for the density of the nucleus $N\rho_d$ is of the order of the mean density of the giant molecular clouds. We can speculate that the density of the original supercloud's nucleus was enhanced during the pass through the Perseus arm (see Section 5). If we assume that, about 60 Myr ago, the ellipsoid representing the nucleus had a semimajor axis of 70 pc, the nucleus' mass was ≈2 × 10^6 M$_\odot$, which is compatible with the masses estimated for Gould's belt (see table 2 of Bobylev 2014). Therefore, we can neglect the gravitational influence of the nucleus on the more extended stellar component of the supercloud (i.e. Stream II).

In order to trace back in time the orbit of the nucleus and of Stream I, we should solve equations (24) and (25). We do not know observationally all initial conditions of the hypothetical nucleus and of Stream I, as well as, the expressions for the force components N_η and N_ξ. Nevertheless, by making use of certain contour conditions, it will be able to obtain values for these unknowns. We assume that the LSR velocity of the nucleus and of the supercloud's centre are both at the present null, and consequently $\dot{X}_N^\star(LSR) = 0$ and $\dot{Y}_N^\star(LSR) = 0$. Thus, the initial relative velocities of the nucleus depend only on the initial position, namely: $\dot{\eta}_N^\star(0) = -\omega_0 \xi_N^\star(0)$ and $\dot{\xi}_N^\star(0) = \omega_0 \eta_N^\star(0)$ (cf. equation A3). Therefore, we here have two unknowns, $\eta_N^\star(0)$ and $\xi_N^\star(0)$.

The spatial distributions of Streams I and II are not well know. These two stellar streams are surely extended structures. At least, we can say that, within a relatively small radius around the Sun, both stellar streams are inter-penetrated. Hence, we will adopt as an approximation that the centroids of the both spatial distributions coincide at the present, i.e. at $t = 0$. Therefore, $\eta_I^\star(0) = \eta_{II}^\star(0) = 569.3$ pc and $\xi_I^\star(0) = \xi_{II}^\star(0) = -218.1$ pc (see Section 3.1) and the initial position we need to solve equation (25) is related with the

initial position of the nucleus, which we do not know, by means of $\eta_I^{\star\star}(0) = \eta_I^\star(0) - \eta_N^\star(0)$ and $\xi_I^{\star\star}(0) = \xi_I^\star(0) - \xi_N^\star(0)$.

From the velocity distribution of nearby stars determined by Bovy et al. (2009); Bovy & Hogg (2010), we obtain that the X and Y components of the LSR velocity centroid of Stream I are ≈ -10 km s^{-1} and $+15$ km s^{-1}, respectively, and therefore $\dot{X}_I^\star(\text{LSR}) = -10$ km s^{-1}, and $\dot{Y}_I^\star(\text{LSR}) = +15$ km s^{-1}. This velocity centroid of Stream I was estimated by eye on fig. 1 of Bovy & Hogg (2010), as described in Section 3.1 for Stream II. Substituting the resulting expressions for the initial position of Stream I and supposing that the nucleus is at rest in the LSR system, we get from equations (A6) the initial relative velocity of Stream I, which only depends on two unknowns, namely: the position components of the nucleus, $\eta_N^\star(0)$ and $\xi_N^\star(0)$.

Here, our premise is that the average position and velocity of Stream I and of Stream II are coincident with the position and velocity of the nucleus's centre at the time $t = -60$ Myr. This imposes eight conditions that the solutions of equations (24) and (25) must satisfy, namely:

$$\eta_I^{\star\star}(t_d') = 0$$
$$\xi_I^{\star\star}(t_d') = 0$$
$$\dot{\eta}_I^{\star\star}(t_d') = 0$$
$$\dot{\xi}_I^{\star\star}(t_d') = 0$$
$$\eta_N^\star(t_d') = \eta_{II}^\star(t_d')$$
$$\xi_N^\star(t_d') = \xi_{II}^\star(t_d')$$
$$\dot{\eta}_N^\star(t_d') = \dot{\eta}_{II}^\star(t_d')$$
$$\dot{\xi}_N^\star(t_d') = \dot{\xi}_{II}^\star(t_d') \tag{26}$$

where $t_d' = -60$ Myr. This system of equations will allow us to solve for eight unknowns. On the side of the initial conditions we have two unknowns, then we have room for assigning to the force components, N_η and N_ξ, three free parameters each. Consequently, we define $N_\eta = N\eta_0 + N\eta_1\, t + N\eta_2\, t^2$ and $N_\xi = N\xi_0 + N\xi_1\, t + N\xi_2\, t^2$. The solution of equation (24) can be obtained from the power-series solutions given by equations (20), (21) and (22), replacing F_η and F_ξ by $f\eta_0 - N_\eta$ and $f\xi_0 - N_\xi$, respectively. Similarly, replacing F_η and F_ξ by N_η and N_ξ, respectively, and the corresponding fixed parameters (i.e. k_N and λ_N), we obtain the solution of (25). These solutions are functions of the eight unknowns (i.e. $\eta_N^\star(0)$, $\xi_N^\star(0)$, $N\eta_0$, $N\eta_1$, $N\eta_2$, $N\xi_0$, $N\xi_1$ and $N\xi_2$) and of the time t. Since these solutions must satisfy the conditions (26) at $t_d' = -60$ Myr, we have a linear system of eight equations with eight unknowns, whose solution gives $\eta_N^\star(0) = 718.5$ pc, $\xi_N^\star(0) = -140.3$ pc, $N\eta_0 = -0.637$ km s^{-1} Myr^{-1}, $N\eta_1 = -0.109$ km s^{-1} Myr^{-2}, $N\eta_2 = -0.002$ km s^{-1} Myr^{-3}, $N\xi_0 = -1.146$ km s^{-1} Myr^{-1}, $N\xi_1 = -0.192$ km s^{-1} Myr^{-2} and $N\xi_2 = -0.004$ km s^{-1} Myr^{-3}. Thus, the force components N_η and N_ξ are given by $N_\eta = -0.637 - 0.109\,t - 0.002\,t^2$ and $N_\xi = -1.146 - 0.192\,t - 0.004\,t^2$; which are plotted in Fig. 8. The values of these force components are both negative between -50 and -60 Myr. Therefore, in this time interval, the direction of N_η is opposite to the direction of the Galactic rotation and N_ξ points to the Galactic centre. Interestingly, the direction of the resultant force $(N_\eta + N_\xi)$ is similar to the direction of the Big Dent's elongation (see Fig. 7).

From the found parameters, we now are in conditions to calculate the orbit of the nucleus's centre, as well as the orbit of Stream I as a whole with respect to its gaseous component (i.e. the supercloud's nucleus) and with respect to the supercloud's centre. Figs 9 and 10 display the orbit and orbital velocities of the Stream I's barycenter with respect to the centre of the supercloud's nucleus.
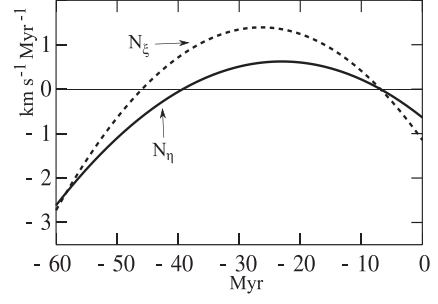

Figure 8. The force components N_η (full line) and N_ξ (dashed line), exerted on the supercloud's gaseous nucleus, as functions of time.
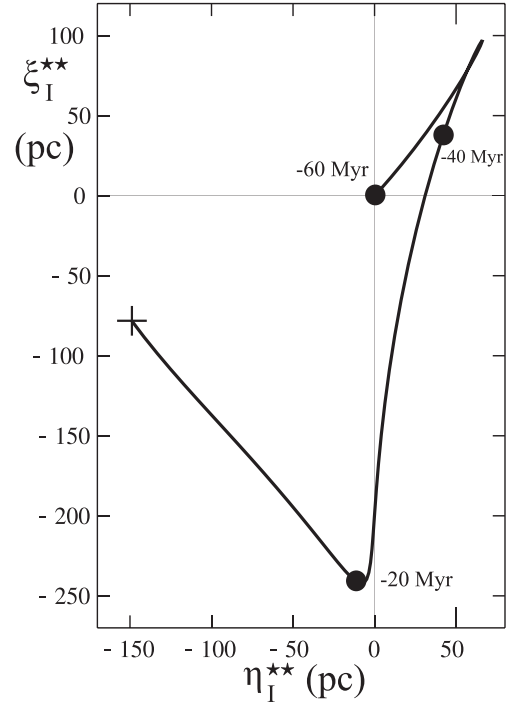

Figure 9. Orbit of Stream I relative to the centre of the gaseous nucleus of the supercloud. The points show positions at the indicated times

The Stream I's orbit referred to the supercloud's centre is shown in Fig. 11, together with the orbit of the gaseous nucleus and with the Stream II's orbit calculated in the previous section. Assuming that the present position of the gaseous nucleus's centre is coincident with the centre of Lindblad's ring (Lindblad 1967) related to Gould's belt, we will be able to find the position of the Sun with respect to the present position of the supercloud's centre. Given the distance and the Galactic longitude to the centre of Lindblad's ring, $d_G = 166$ pc and $L_G = 131°$ (see table 1 of Olano 1982), we can write $\eta_\odot^\star = \eta_N^\star(0) - d_G \sin L_G$ and $\xi_\odot^\star = \xi_N^\star(0) + d_G \cos L_G$, resulting $\eta_\odot^\star = 593$ pc and $\xi_\odot^\star = -249$ pc (see Fig. 11). In Fig. 12, we show the orbit of the supercloud nucleus in the Galactocentric system $(\tilde{x}, \tilde{y})$, that is to say relative to the spiral arms, for which we have converted the positions $(\eta_c(t) + \eta_N^\star(t), \xi_c(t) + \xi_N^\star(t))$ into positions $(\tilde{x}, \tilde{y})$ (see Section 3.1). Note that, according to Fig. 12, the nucleus moved in the time interval of ≈ -30 Myr to -20 Myr within the internal edge of the Sagittarius-Carina arm.
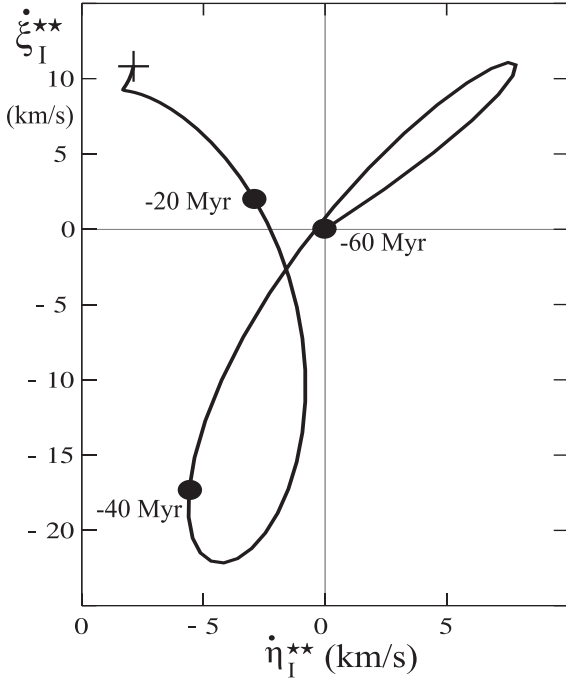
Figure 10. The velocity components along the orbit of Stream I, as a whole, relative to the centre of the gaseous nucleus of the supercloud. The points show velocities at the indicated times.
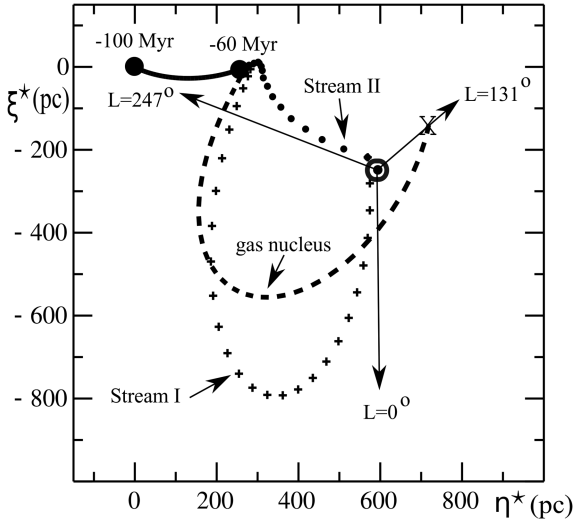
Figure 11. Orbits relative to the supercloud's centre of its three subsystems: Stream I (crosses), Stream II (points) and the supercloud's nucleus (dashed line). The shared orbit is indicated by a full line. The symbol X denotes the present position of the gas nucleus, which is considered to be coincident with the centre of Lindblad's ring, associated with Gould's belt (Olano 1982). The Sun's position (Sun symbol) and three Galactic directions are indicated.
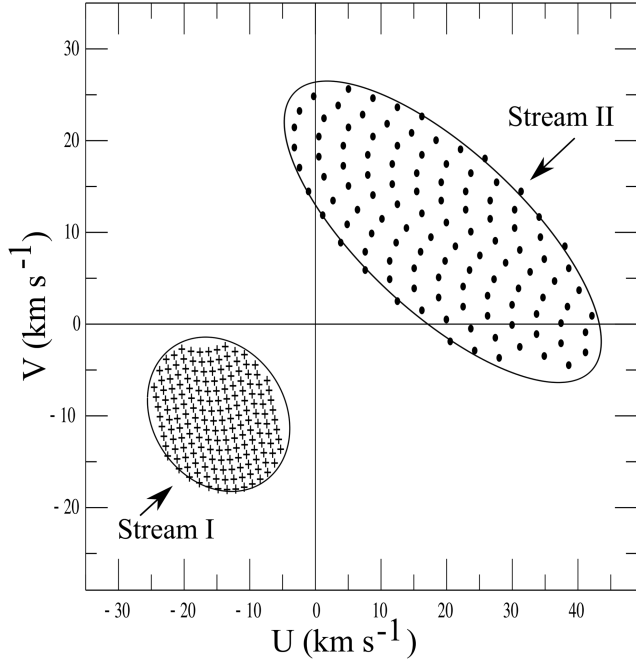
4 SPATIAL AND VELOCITY DISTRIBUTIONS OF STREAMS I AND II, AS PREDICTED BY THE MODEL

On the basis of our model, we have calculated the respective orbits of Stream I and II as a whole. The aim of this section is to generate an overall theoretical distribution of the present stellar positions and velocities for Stream I and for Stream II. With this purpose, we will assume that the stars of Stream II had a certain spatial and velocity
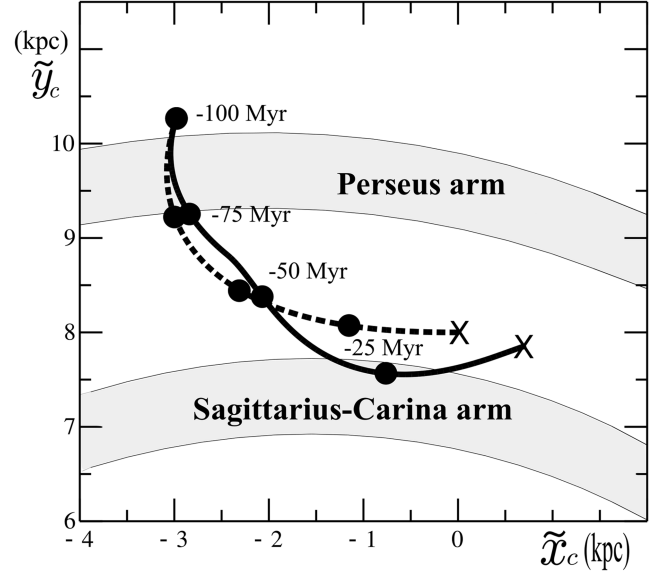

Figure 12. Orbit of the supercloud's centre (dashed line) and of its gaseous nucleus (full line), relative to the nearly spiral arms of the Galaxy. This figure is the same as Fig. 5, except we have here included the orbit of the gaseous nucleus and the orbit of the supercloud's centre is here represented by a dashed line.

distribution at the moment when the mean position and velocity of gas and stars agreed (i.e. 100 Myr ago), and similarly for the stars of Stream I (i.e. 60 Myr ago). Here, it is convenient to calculate orbits forward in time, and therefore we will use the positions and velocities that stars of Streams I and II had 60 and 100 Myr ago, respectively, as the initial conditions ($t = 0$). Hence, with $t = 60$ and $t = 100$ Myr, we obtain the present positions and velocities of the Stream I stars and of the Stream II stars, respectively. With respect to the initial distribution of positions and velocities of the stars, we will distinguish three cases: (A) the stars rotated clockwise circularly around an axis that passes through the gas cloud's centre and is perpendicular to the Galactic plane; (B) the stars rotated counterclockwise circularly around the mentioned rotation axis; (C) the LSR velocities of the stars relative to the gas cloud's centre were randomly distributed according to a Gaussian uniform distribution, with a mean velocity equal to zero and a velocity dispersion σ_v equal to that derived from the Virial theorem: namely, $\sigma_v = \sqrt{\frac{GM}{2a}}$, and therefore $\sigma_v = 12.4$ km s^{-1} for Stream II and 8.7 km s^{-1} for Stream I. In the three cases, the space distribution of the stars (or number density of stars) is considered uniform over the cloud. The circular velocity of rotation is given by $v_c = -k\,r$ for case A, $v_c = k\,r$ for case B, from which we calculate the initial velocity components of the mass points representing the stars (see Olano 2015). When calculating v_c for Stream I, we use k_N instead of k. In our simulation, the initial positions of the points representing the stars are regularly spaced on the inner equatorial plane of the gas cloud. Assigning to each initial position the corresponding velocity components, and using the motion equations and the values of the parameters of Section 3.1 for Stream II and of Section 3.2 for Stream I, we calculate the orbits of all those mass points representing the stars. The resulting theoretical distributions of the present velocities and positions of both streams are shown in Figs 13 and 14 for Case A, Figs 15 and 16 for Case B, and Figs 17 and 18 for Case C. The velocities are all relative to the LSR system and represented in the U-V kinematic plane (Figs 13, 15 and 17), which is useful to compare with the
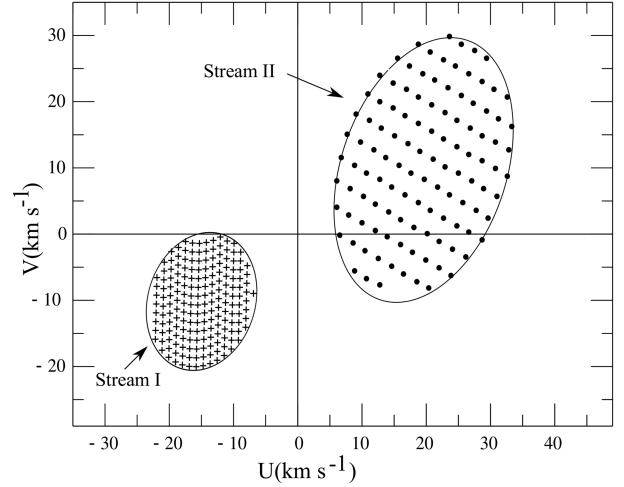
Figure 13. Theoretical velocity distribution for Case A. The velocities U and V are referred to the LSR system. The crosses and points represent stars of Stream I and II, respectively.
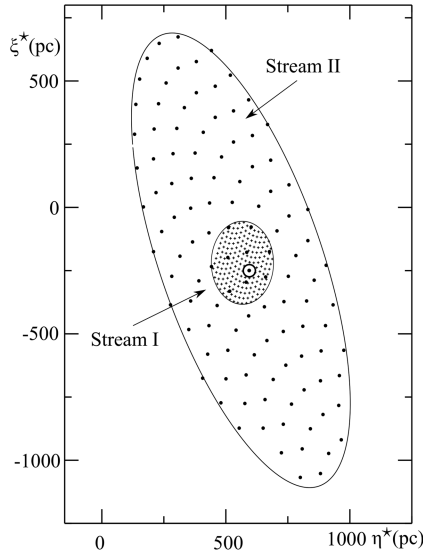
Figure 14. Theoretical spatial distributions for Case A. The crosses and points represent stars of Stream I and II, respectively. The Sun symbol indicates the position of the Sun.

Figure 15. Theoretical velocity distribution for Case B. The velocities U and V are referred to the LSR system. The crosses and points represent stars of Stream I and II, respectively.
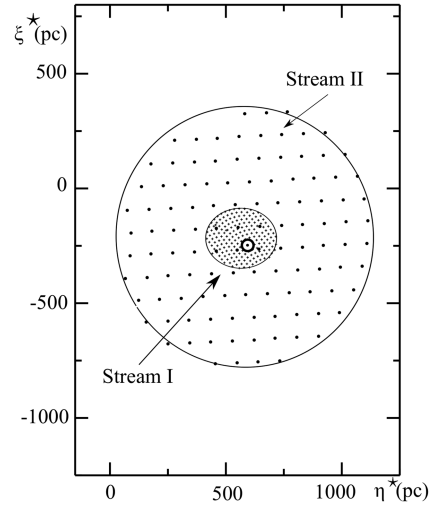

Figure 16. Theoretical spatial distributions for Case B. The crosses and points represent stars of Stream I and II, respectively. The Sun symbol indicates the position of the Sun.

observational velocity distributions (e.g. Bovy et al. 2009; Gontcharov 2012a,b). The positive U-axis points towards the galactic longitude $l = 0°$, and the positive V-axis towards $l = 90°$. In order to convert our LSR velocity components into the corresponding components U and V, we should have into account that our components $\dot{X}_I$(LSR) and $\dot{X}_{II}$(LSR) agree with the respective components V and that our components $\dot{Y}_I$(LSR) and $\dot{Y}_{II}$(LSR) coincide with the respective components U, but with reversed sign.

Our simulations show that a spherical velocity distribution of the Stream stars, given at the beginning, is transformed into an ellipsoidal one. This is particularly clear for Stream II. The longitude difference Δl between the major axis of the velocity ellipse and the direction to the galactic centre is called the deviation of the vertex. $\Delta l \approx 47°$ in Case A for Stream II (Fig. 13), which is approximately coincident with its observed deviation of the vertex (cf. figs 1 and 6 of Bovy & Hogg 2010; Gontcharov 2012b). The distributions obtained for Case C (Figs 17 and 18) are similar to those for Case A, but with a minor enhancement of the ellipsoidal characteristic of the distributions. In contrast, the deviation of the vertex of Stream II in Case B (Fig. 15) is very differ from the observed one. Therefore, the conditions of Case B should be discarded. Even though, we have used an initial uniform spatial distribution of the Stream stars, it is easy to infer, from the observed velocity distribution of Stream II, that the stars of Stream II were more concentrated radially towards the gas cloud's centre. However, the initial spatial distribution of the stars of Stream I was not so regular, judging from the present existence of at least three concentrations of stars in the phase space (position-velocity).
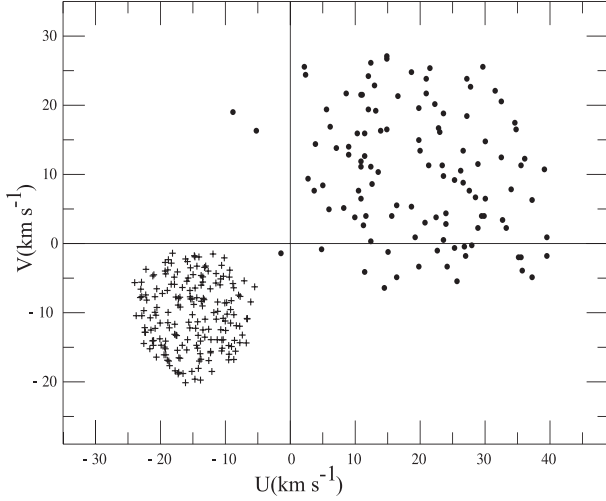
Figure 17. Theoretical velocity distribution for Case C. The velocities U and V are referred to the LSR system. The crosses and points represent stars of Stream I and II, respectively.
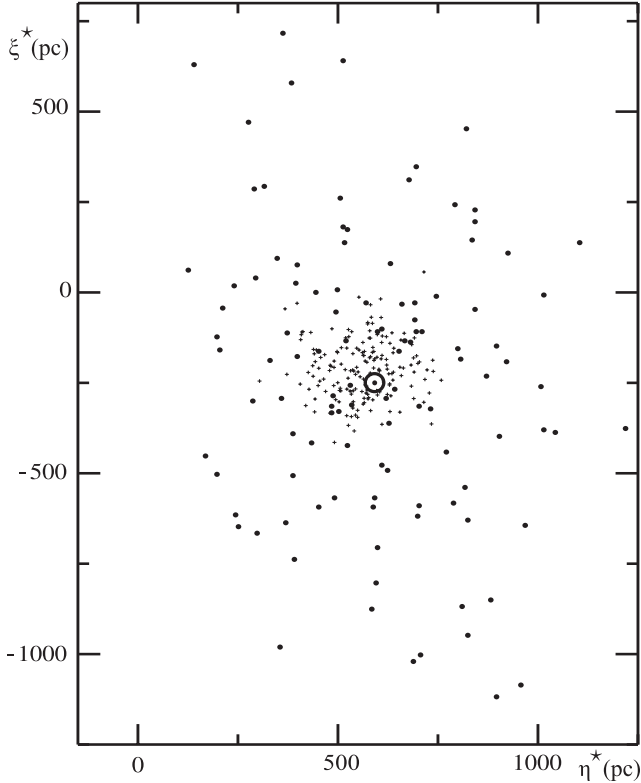

Figure 18. Theoretical spatial distributions for Case C. The crosses and points represent stars of Stream I and II, respectively. The Sun symbol indicates the position of the Sun.

Let me mention some of the limitations that difficult the comparison between the theoretical and observational distributions. The observational spatial distributions of Streams I and II are not well known. Fig. 14 shows that the spatial distribution of Stream II would be rather widespread, and therefore a representative sample to obtain observationally the stellar velocity distribution of Stream II should include stars within a radius of at least 1000 pc from the Sun. Gontcharov (2012a), based on a sample of 20 514 stars,

obtained the spatial distribution of stars within a radius of 600 pc, and interestingly his Fig. 3 shows that, although the spatial distributions of Stream I and II are not discriminated, the stars that can belong to Stream I and/or Stream II fill the studied volume. Note that Gontcharov (2012a) used the Galactic coordinate system (X,Y,Z). Then, the *X*-axis coincides with our $\xi^\star$-axis, but the positive *X*-axis is directed towards the Galactic centre. The *Y*-axis and our $\eta^\star$-axis coincide and point in the same direction. Besides, the origin of the system (X,Y,Z) is at the Sun, while the origin of our system ($\eta^\star$, $\xi^\star$) is at the centre of the supercloud (Figs 14, 16 and 18). On the other hand, apart from we have used a highly idealized gravitational potential for the clouds, we have considered only stars whose orbits remained within the physical boundaries of the clouds, and excluded those stars that, even gravitationally bounded to the clouds, exceeded the bounds of the clouds.

5 DISCUSSION OF THE RESULTS: UNCERTAINTIES OF THE FITTED PARAMETERS OF THE MODEL

In the previous section, we have used as a first approximation a linear relationship for the temporal variation of the mean density of the supercloud and of its nucleus, which is determined from the cloud's characteristic density at the beginning of the disintegration process and from a relatively low density at the end of this process. We can assume that this density variation is essentially due to the clouds' pure expansion, ignoring details of the expansion law. On the other hand, we have found that probably the supercloud penetrated the Perseus arm and that the nucleus was strongly perturbed. Therefore, we should also consider the possibility that these clouds accreted significant quantities of mass during a period of $\approx$10–20 Myr. If $M(t)$ and $V(t)$ denote the mass and the volume of the cloud in question at the time t, by definition the cloud's mean density at this time is $\rho(t) = \frac{M(t)}{V(t)}$. We will represent the temporal variation of the cloud's mass as $M(t) = M(0)(1 + \gamma \exp(-\beta(t - t_d))$, where M(0) is the mass at t = 0, $\gamma = \frac{M(t_d)-M(0)}{M(0)}$, $M(t_d)$ is the cloud's mass at $t = t_d$ and β characterises the time interval of accretion. We assume that $V(t) = \frac{4}{3}\pi a(t)^3 \sqrt{1 - e^2}$, the cloud's volume that corresponds to that of an ellipsoid of semimajor axis $a(t)$ and that expands homologously. We will represent the expansion law of the supercloud by a quadratic function of the form $a(t) = a_0 (1 + \mu_1 t + \mu_2 t^2)$, where $a_0 = a(0)$. The values of the coefficients μ_1 and μ_2 are derived from the values adopted for a at the present (a_0), at the time $t_g = -60$ Myr (a_g) and at $t_d = -100$ Myr (a_d). Since $M(0) = \frac{4}{3}\pi\rho_0 a_0^3 \sqrt{1 - e^2}$,

$$\rho(t) = \rho_0 \frac{(1 + \gamma \exp(-\beta(t - t_d)))}{(1 + \mu_1 t + \mu_2 t^2)^3}, \qquad (27)$$

where $\rho_0 = \rho(0)$. In order to solve analytically the motion equations with the temporal density variation of equation (27), this equation can be approximated by a polynomial of high degree or an expansion in power series

$$\rho(t) = \rho_0 \left(1 + \sum_{n=1}^{\infty} \rho_n t^n \right), \qquad (28)$$

(see Appendix B). Now, we are in conditions to evaluate the effects of a non-linear relationship for $\rho(t)$ on the model's results.

We adopt as an example $\gamma = -0.5$, which implies that the original mass of the supercloud $M(t_d)$ increased by a factor of 2 as consequence of the accretion. If we adopt $M(t_d) = 2.5\ 10^7\ M_\odot$, which lies within the range of supercloud's mass, and for the present average
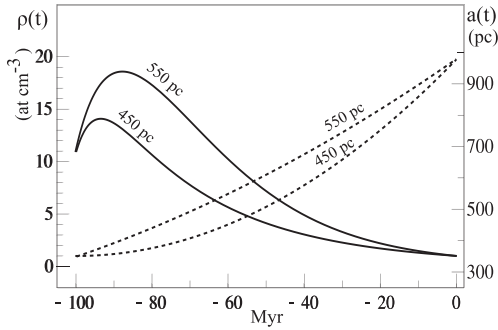
Figure 19. The mean density (full lines) and semimajor axis (dashed lines) of the supercloud as a function of time. The numbers on the curves indicate the corresponding values of the semimajor axis at $t = -60$ Myr (i.e. a_g).

density of the supercloud $\rho_0 = 1$ at cm^{-3}, a typical ISM density, we obtain that $a_0 = 1000$ pc. Besides, we assume $a_d = 350$ pc, which lies within the range of the supercloud's radius. We will keep fixed the above parameters, including $\beta = 0.15$, but we will vary a_g between 450 and 550 pc. The function $\rho(t)$ is shown in Fig. 19. By means of the method of Section 3.1 and of the solutions given in Appendix B, and using the adopted set of parameters that determines $\rho(t)$, namely: $\rho_0 = 1$ at cm^{-3}, $\gamma = -0.5$, $\beta = 0.15$, $a_0 = 1000$ pc, $a_d = 350$ pc and $a_g = 500 \pm 50$ pc, we obtained that $\eta_{II}^\star(0) = 691_{+60}^{-40}$ pc, $\xi_{II}^\star(0) = -195_{+130}^{-120}$ pc, $F_\eta = f\eta_0 = -0.40_{-0.04}^{+0.02}$ km s^{-1} Myr^{-1} and $F_\xi = f\xi_0 = 0.38_{+0.04}^{-0.02}$ km s^{-1} Myr^{-1}. The new values obtained for the free parameters of the model do not differ significantly from those obtained in Section 3.1 and therefore the corresponding orbits of the supercloud and Stream II are similar to those represented in Figs 2, 4, 5 and 7. We should say that we have greatly simplified the expansion process of the supercloud in our model, ignoring among other things that, due to the Galactic rotation differential, the supercloud was elongated as well. This elongated structure would have formed the local arm. The respective gaseous configurations of the Orion arm and of Gould's belt are both similar to that of an elongated expanding ring of gas (Lindblad 1967; Olano 1982, 2001).

Using modern determinations of Ω_p, we have found that the supercloud would have crossed the Perseus arm and only passed tangentially through the internal edge of the Sagittarius-Carina arm (see Fig. 12). However, if we use the classical values of Ω_p (≈ 12 km s^{-1} kpc^{-1}), the encounter of the supercloud in the considered period is *entirely* with the Sagittarius-Carina arm. In our model, we have considered that the stellar spatial distribution of Stream II (Sirius group) covered the whole supercloud, while that the stars of Stream I were associated with the supercloud's nucleus, region with the highest gas density. However, in principle, we can invert the roles of Streams I and II, resulting in this case that supercloud comes from the Sagittarius-Carina arm. The observation of the spatial distributions of Streams I and II would help to decide between the two possibilities. If Stream II's distribution is more extended than Stream I (see Figs 14, 16 and 18), then the roles assigned to Streams I and II by our model would be correct. On the other hand, the orbit determined with the assumptions of the model suggests connections with other interesting facts of the local Milky Way as the Big Dent (Alfaro et al. 1991), (see Fig. 7), and the huge hole in the distribution of the local interstellar matter, towards the galactic longitude of about $l = 240°$ (see Fig. 11). Perhaps, this gas hole is in part a consequence of the event that originated the Big Dent and Gould's belt.

6 CONCLUSIONS

We have developed epicyclic equations to study the motion of an interstellar gas cloud in an arbitrary Galactic orbit, and the drift of its stellar component, when the cloud is subjected to non-gravitational additional forces. By means of these epicyclical motion equations and initial and boundary conditions, provided both by observational data and model's assumptions, we have traced back in time the orbits of the local supercloud and of the associated stellar Streams, I and II.

The results indicate that before 100 Myr ago the supercloud would have had a relatively high velocity peculiar of 30–40 km s^{-1}, which favours the possibility that the supercloud contained an important percentage of captured field stars (Olano 2015). We also have found that the supercloud could have interacted with the Perseus arm between 75–100 Myr ago (Fig. 5), explaining in part the strong braking that the gas component of the supercloud suffered since then. Since the stars were not greatly affected by the interaction with the background interstellar medium, the stars of Streams I and II tended to conserve the kinematics originally shared with the gas component of the supercloud.

Another interesting fact indicated by the supercloud's orbit is that about 60 Myr ago the supercloud and the so-called Big Dent (Alfaro et al. 1991) were located approximately on the same Galactic region (Fig. 7). Therefore, we can not discard that the supercloud may have played an active role in the origin the Big Dent. Even though we did not study the vertical motion of the supercloud, a possibility is that the crossing of the supercloud throughout the Galactic plane deformed the Galactic layer forming the big depression named Big Dent. However, we think that the main role may have been played by a contingent event, such as the falling of a HVC (Olano 2004, 2008, and references therein), that affected to both the supercloud and the surrounding Galactic layer. These two mechanisms for the origin of the Big Dent could also explain the expansion of the supercloud, which in turn originated the Orion arm, and the origin of Gould's belt, which occurred about 60 Myr ago. In other words, the three subsystem of gas and stars; namely, the Big Dent, the Orion arm and Gould's belt, may have had a common origin.

With the purpose of explaining the spatial and velocity distributions of Streams I and II, we have assumed that the stars of Stream II were originally distributed throughout the whole supercloud, while the stars of Stream I were concentrated within a supercloud's region of relatively high gas density, we have denominated the supercloud's nucleus. Besides, we have assumed that an event, such as a cloud–cloud collision, occurred about 60 Myr ago and probably in part related to the larger scale phenomenon that generated the Big Dent, perturbed strongly the gas nucleus of the supercloud giving origin to Gould's belt and as a consequence affected the kinematics of Stream I. Simulations based on the supercloud's model allow us to obtain the spatial and velocity distributions for Streams I and II, where two of which (Figs 13, 14 and Figs 17, 18) result in principle compatible with the observational ones.

The epicyclic formulation developed in this paper can be an appropriate tool to study the problem of capture of field stars when an interstellar gas cloud gets a peculiar velocity. These epicyclic motion equations give a better approximation than the supposition of a linear acceleration or deceleration of the cloud (Olano 2015). The hypothesis of the local supercloud has given us an insight into the complex processes that may have led to the formation of the local system, and and can guide us through future observational and theoretical efforts. Further observational studies, such as the determination of the global spatial distribution of

Stream I and II, will be useful to contrast the hypothesis of the local supercloud.

For example, the ample study by Gontcharov (2012a) that is based on a complete and homogeneous data set including proper motions and radial velocities could be extended to include stars of the local disc with different spectral types and with distances from the Sun greater than 600 pc, which will be of interest for the purposes of the present investigation program. To represent separately the spatial distributions of Streams I and II, we should simply select the spatial positions of those stars lying in the age and velocity ranges that characterize the stream in study (i.e. Stream I or II). Bobylev (2014), in the conclusions of his review, pointed out some problems on the structure, dynamics and evolution of the local system that we should address and observational projects that will provide high–precision data and that will help us to solve these problems.

We have focused our investigation on the motions of the supercloud and of the two stellar streams parallel to the Galactic plane. Then, the next step should be to address the problem of their motions in the z-direction, perpendicular to the Galactic plane. Since the z-motions are decoupled from the other motion components, in principle, we can try them independently. The study of the z-motions of the local subsystems could shed light on the processes that deformed in the z-direction the local Galactic layer (the Big Dent) and led the origin of Gould's belt.

ACKNOWLEDGEMENTS

REFERENCES

Alfaro E. J., Cabrera-Caño J., Delgado A. J., 1991, ApJ, 378, 106
Bobylev V. V., 2014, Astrophysics, 57, 583
Bobylev V. V., Bajkova A.T, Mylläri A. A., 2010, Astron. Lett., 36, 27
Bok B. J., 1934, Harvard Circ., 384, 1
Bovy J., Hogg D. W., 2010, ApJ, 717, 617
Bovy J., Hogg D. W., Roweis S. T., 2009, ApJ, 700, 1794
Bovy J. et al., 2012, ApJ, 759, 131
Cabrera-Caño J., Moreno E., Franco J., Alfaro E. J., 1995, ApJ, 448, 149
Chandrasekhar S., 1942, Principles of Stellar Dynamics. Dover Publications, New York
Clube S. V. M., Napier W. N., 1982, QJRAS, 23, 45
Clube S. V. M., Napier W. N., 1986, in Smoluchowki R., Bahcall J. N., Mattews M. S., eds, The Galaxy and the Solar System. The Univ. Arizona Press, Tucson, p. 69
Comerón F., Torra J., 1992, A&A, 261, 94
de la Fuente Marcos R., de la Fuente Marcos C., 2004, New Astron., 10, 53
De Simone R. S., Wu X., Tremaine S., 2004, MNRAS, 350, 627
Dehnen W., 1998, AJ, 115, 2384
Efremov Yu. N., 2010, MNRAS, 405, 1531
Eggen O. J., 1998, AJ, 116, 782
Elmegreen B. G., Elmegreen D. M., 1983, MNRAS, 203, 31
Famaey B., Jorissen A., Luri X., Mayor M., Udry S., Dejonghe H., Turon C., 2005, A&A, 430, 165
Famaey B., Siebert A., Jorissen A., 2008, A&A, 483, 453
Gontcharov G. A., 2012a, Astron. Lett., 38, 694
Gontcharov G. A., 2012b, Astron. Lett., 38, 771
Junqueira T. C., Chiappini C., Lépine J. R. D., Minchev I., Santiago B. X., 2015, MNRAS, 449, 2336
Kapteyn J. C., 1905, Star Streaming, Report of the British Association for the Advancement of Science, South Africa, p. 257
Lindblad B., 1941, Stockholms Observatoriums Annaler, 13, 10.1
Lindblad P. O., 1967, Bull. Astron. Inst. Neth, 19, 34
Mineur H., 1939, Ann. d'ap., 2, 1
Monguió M., Grobøl P., Figueras F., 2015, A&A, 577, A142
Navarro J. F., Helmi A., Freeman K. C., 2004, ApJ, 601, L43
Olano C. A., 1982, A&A, 112, 195
Olano C. A., 2001, AJ, 121, 295
Olano C. A., 2004, A&A, 423, 895
Olano C. A., 2008, A&A, 485, 457
Olano C. A., 2015, MNRAS, 447, 3016
Pöppel W. G. L., 1997, Fund. Cosm. Phys.,18, 1
Roberts W. W., 1969, ApJ, 158, 123
Sofue Y., Honma M., Omodaka T., 2009, PASJ, 61, 227
Torra J., Fernández D., Figueras F., 2000, A&A, 359, 82
Vallée J. P., 2014, ApJS, 215, 1

APPENDIX A: RELATIVE MOTION EQUATIONS OF THE SUPERCLOUD'S NUCLEUS AND OF STREAM I

(a) The relative motion of the supercloud's nucleus with respect to the supercloud's centre. We suppose that the supercloud contained a gaseous nucleus of density much greater than the mean density of the supercloud. Hence, the dynamics of the nucleus is different from the rest of the supercloud's gaseous component. Besides, we assume that, in the evolutionary course of the supercloud, the nucleus was involved by a very energetic process that affected its orbit. If the nucleus is subject to the gravitational forces of the supercloud, whose components are denoted by J_η and J_ξ, and to a non-gravitational force of components N_η and N_ξ, the motion equations of the nucleus in the rotating system (η, ξ) can be written

$$\ddot{\eta}_N + 2\omega_0 \dot{\xi}_N = J_\eta + N_\eta$$
$$\ddot{\xi}_N - 2\omega_0 \dot{\eta}_N - 2\omega_0^2 \xi_N = J_\xi + N_\xi \tag{A1}$$

(cf. equations 14 and 15). Making use of the relationships $\eta_N^\star(t) = \eta_N(t) - \eta_c(t), \xi_N^\star(t) = \xi_N(t) - \xi_c(t)$, equations (A1), (12) and (13), we can write the equations for the motion of the nucleus about the supercloud's centre as follows

$$\ddot{\eta}_N^\star + 2\omega_0 \dot{\xi}_N^\star = J_\eta + N_\eta - F_\eta$$
$$\ddot{\xi}_N^\star - 2\omega_0 \dot{\eta}_N^\star - 2\omega_0^2 \xi_N^\star = J_\xi + N_\xi - F_\xi. \tag{A2}$$

Substituting $J_\eta = -k^2(1 + \lambda t)\eta_N^\star$ and $J_\xi = -k^2(1 + \lambda t)\xi_N^\star$, equations (A2) become into equations (24). The initial velocities we need to solve the system of equations (A2) or (24) are related with the initial positions and the LSR velocities of the nucleus and of the supercloud's centre in the following way

$$\dot{\eta}_N^\star(0) = -\omega_0 \xi_N^\star(0) + \dot{X}_N^\star(\text{LSR})$$
$$\dot{\xi}_N^\star(0) = \omega_0 \eta_N^\star(0) + \dot{Y}_N^\star(\text{LSR}), \tag{A3}$$

where $\dot{X}_N^\star(\text{LSR}) = \dot{X}_N(\text{LSR}) - \dot{X}_c(\text{LSR})$ and $\dot{Y}_N^\star(\text{LSR}) = \dot{Y}_N(\text{LSR}) - \dot{Y}_c(\text{LSR})$.

(b) The relative motion of Stream I with respect to the supercloud's nucleus. We propose that the stars of Stream I have been gravitationally attached to the gaseous nucleus of the supercloud. By similarity with equations (14) and (15), we can write

$$\ddot{\eta}_I + 2\omega_0 \dot{\xi}_I = J_\eta + NJ_\eta$$
$$\ddot{\xi}_I - 2\omega_0 \dot{\eta}_I - 2\omega_0^2 \xi_I = J_\xi + NJ_\xi \tag{A4}$$

where NJ_η and NJ_ξ are the components of the force exerted on Stream I by the supercloud's nucleus. By resting term by term the corresponding equations of (A4) and (A1) and defining

$\eta_I^{\star\star}(t) = \eta_I(t) - \eta_N(t)$ and $\xi_I^{\star\star}(t) = \xi_I(t) - \xi_N(t)$, we obtain the equations for the motion of Stream I around the nucleus:

$$\ddot{\eta}_I^{\star\star} + 2\omega_0\,\dot{\xi}_I^{\star\star} = NJ_\eta - N_\eta$$

$$\ddot{\xi}_I^{\star\star} - 2\omega_0\,\dot{\eta}_I^{\star\star} - 2\omega_0^2\,\xi_I^{\star\star} = NJ_\xi - N_\xi. \tag{A5}$$

Note that the force components J_η and J_ξ are here cancellated. Adopting a force law similar to that of the supercloud as a whole, we can write $NJ_\eta = -k_N^2(1 + \lambda_N\,t)\,\eta_I^{\star\star}$ and $NJ_\xi = -k_N^2(1 + \lambda_N\,t)\,\xi_I^{\star\star}$, with which we get equations (25). The initial relative velocities of Stream I are given by the following relationships:

$$\dot{\eta}_I^{\star\star}(0) = -\omega_0\,\xi_I^{\star\star}(0) + \dot{X}_I^{\star\star}(\mathrm{LSR})$$

$$\dot{\xi}_I^{\star\star}(0) = \omega_0\,\eta_I^{\star\star}(0) + \dot{Y}_I^{\star\star}(\mathrm{LSR}), \tag{A6}$$

where $\dot{X}_I^{\star\star}(\mathrm{LSR}) = \dot{X}_I(\mathrm{LSR}) - \dot{X}_N(\mathrm{LSR})$ and $\dot{Y}_I^{\star\star}(\mathrm{LSR}) = \dot{Y}_I(\mathrm{LSR}) - \dot{Y}_N(\mathrm{LSR})$.

APPENDIX B: SOLUTION OF THE MOTION EQUATIONS FOR A NON-LINEAR TEMPORAL VARIATION OF THE CLOUD'S DENSITY

If the temporal variation of the cloud's density is expressed in power series by equation (28), the term $(1 + \lambda t)$ of equations (18) should be substituted by $(1 + \sum_{n=1}^{\infty} \rho_n t^n)$. The coefficients of the solution series of equations (18) for $n = 2$ are coincident with equations (21) and for $n \geq 3$ are

$$\eta_n = \frac{1}{n(n-1)}\left(-f\eta_{n-2} - k^2\sum_{i=1}^{n-2}\rho_i\,\eta_{n-2-i} - k^2\eta_{n-2} \right.$$
$$\left. - 2(n-1)\omega_0\xi_{n-1} \right)$$

$$\xi_n = \frac{1}{n(n-1)}\left(-f\xi_{n-2} - k^2\sum_{i=1}^{n-2}\rho_i\,\xi_{n-2-i} - k^2\xi_{n-2} \right.$$
$$\left. + 2(n-1)\omega_0\eta_{n-1} + 2\omega_0^2\xi_{n-2} \right), \tag{B1}$$

where η_0, ξ_0, η_1 and ξ_1 are given by the initial position and velocity.

This paper has been typeset from a TeX/LaTeX file prepared by the author.